J. Am. Soc. Mass Spectrom. (2011) 22:1022–1031
DOI: 10.1007/s13361-011-0121-0

FOCUS: MALDI-TOF AND BIOLOGICAL MS: RESEARCH ARTICLE

High-Speed MALDI-TOF Imaging Mass Spectrometry: Rapid Ion Image Acquisition and Considerations for Next Generation Instrumentation

Jeffrey M. Spraggins,[1,2] Richard M. Caprioli[1,2,3]

[1]Mass Spectrometry Research Center, Vanderbilt University Medical Center, Nashville, TN, USA
[2]Department of Biochemistry, Chemistry, Pharmacology, and Medicine, Vanderbilt University Medical Center, Nashville, TN, USA
[3]Vanderbilt University School of Medicine, 465 21st Avenue South, MRB III Suite 9160, Nashville, TN 37232, USA

Abstract

A prototype matrix-assisted laser desorption ionization time-of-flight (MALDI-TOF) mass spectrometer has been used for high-speed ion image acquisition. The instrument incorporates a Nd:YLF solid state laser capable of pulse repetition rates up to 5 kHz and continuous laser raster sampling for high-throughput data collection. Lipid ion images of a sagittal rat brain tissue section were collected in 10 min with an effective acquisition rate of roughly 30 pixels/s. These results represent more than a 10-fold increase in throughput compared with current commercially available instrumentation. Experiments aimed at improving conditions for continuous laser raster sampling for imaging are reported, highlighting proper laser repetition rates and stage velocities to avoid signal degradation from significant oversampling. As new high spatial resolution and large sample area applications present themselves, the development of high-speed microprobe MALDI imaging mass spectrometry is essential to meet the needs of those seeking new technologies for rapid molecular imaging.

Key words: Mass spectrometry, TOF, MALDI, Imaging, Microprobe, Lipids, Continuous laser raster

Introduction

The emergence of matrix-assisted laser desorption ionization imaging mass spectrometry [MALDI imaging mass spectrometry (IMS)] as a prominent analytical tool [1] has helped drive advancements in instrumentation, lasers, data acquisition methods, and data processing packages. MALDI imaging mass spectrometry began at a time when 20 Hz lasers were standard and acquiring ion images took many hours and even days in some cases to collect data and deal with rough and unproven software. The technology has rapidly developed into a powerful analytical tool able to spatially resolve biologically relevant molecules such as pharmaceuticals, metabolites, lipids, peptides and proteins [2–6], providing a new molecular dimension to classic histology. Technological advancement has been central to the development of MALDI IMS, and developing next generation mass spectrometry instrumentation is essential to expanding its capabilities even further.

MALDI imaging mass spectrometry provides spatially resolved multichannel (m/z) information for intact molecular ions. For biological applications, the experiment is performed by adhering thinly sliced tissue sections onto a target and applying an energy absorbing matrix in a manner that minimizes delocalization of the analyte. Ions are generated as the sample moves through the path of a stationary laser beam and images are constructed by plotting the x and y

Correspondence to: Richard M. Caprioli; *e-mail:* r.caprioli@vanderbilt.edu

Received: 26 January 2011
Revised: 1 March 2011
Accepted: 1 March 2011
Published online: 9 April 2011

coordinates of the ablations spots (pixels) with respect to ion signal intensity as detected by the mass spectrometer. Each pixel contains an entire mass spectrum allowing hundreds of images to be constructed from a single acquisition. This is commonly referred to as microprobe imaging mass spectrometry.

As microprobe MALDI IMS has developed, throughput has been a major issue particularly as the technology advances to higher spatial resolution and larger image areas. For example, a 1 mm^2 tissue section imaged with a spatial resolution of 100 μm produces an image with 100 total pixels, a manageable number of spectra. However, much work is being done to image tissue sections at higher spatial resolutions [7–9] with 5 μm being the current applicable limit for microprobe MALDI IMS. If the same 1 mm^2 tissue section is imaged at 5 μm spatial resolution, 40,000 pixels would be generated taking many hours to acquire. The same consideration applies to sampling larger areas for applications such as determining molecular distributions in whole-body tissue cross sections [10–13] and biomarker discovery using tissue microarrays [14–16]. Developing high-throughput imaging mass spectrometric techniques is essential as MALDI IMS advances.

Laser technology has been central to the evolution of high-speed imaging. MALDI is performed by co-crystallizing or coating the sample with a matrix that efficiently absorbs the energy of the incident laser beam [17]. Matrix molecules often have acidic functionality so that in the plume, following irradiation, protons are efficiently transferred to the analyte resulting in intact protonated molecular ions. Traditionally, N_2 lasers have been used for MALDI imaging, but because of their low repetition rates (50 Hz) these lasers are not ideal for this purpose. Recently, there has been a shift to using frequency tripled solid-state lasers using gain mediums such as Nd:YAG, Nd:YLF, and Nd:YVO_4. Although the Gaussian beam profile for solid-state lasers is not ideal, they have proven effective for MALDI applications and the ability to operate at pulse repetition rates >1 kHz with much longer life spans (typically $>10^9$ shots) than N_2 lasers make them preferred for high-throughput experiments [7, 18]. A recent report described a modified hybrid quadrupole time-of-flight MS with a Nd:YVO_4 laser capable of pulse repetition rates up to 20 kHz [19]. Although higher laser repetition rates were possible, it was reported that operating between 5 and 10 kHz provided the best results, allowing for a 150 μm spatial resolution lipid ion image of a sagittal rat brain tissue section to be acquired in roughly 40 min. This is several times faster than the performance of most commercial MALDI IMS instrumentation.

Traditionally for imaging mass spectrometry experiments, pixels are established by virtually defining an array of discrete spots over the sample area. The sample stage is then moved as to fire the laser a set number of times within the pixel area before moving to the next spot. Often, the laser is turned off when moving between pixels. Recently, continuous laser raster sampling has been introduced as a fast surface interrogation technique that has been shown to reduce ion image acquisition rates by a factor of 5 [20]. The experiment is done by firing the laser continuously as the sample stage is moved in a straight line laterally across the area of interest. Lateral spatial resolution is defined by the laser repetition rate (f_{rep}), sample stage velocity (v_{stage}) and number of laser shots averaged for a single spectrum or pixel [hardware average: (H.A.)] as seen in Eq. 1.

$$\text{Lateral Spatial Resolution} = H.A.\left(\frac{v_{stage}}{f_{rep}}\right) \quad (1)$$

Vertically, spatial resolution is determined simply by the distance between laser raster rows. Although continuous laser raster sampling has been shown to significantly decrease image acquisition time, much has yet to be done to understand the fundamentals of the process. In particular, determining the relationship among continuous laser raster sampling, high repetition rate lasers and data quality is essential in developing next generation high-speed MALDI IMS technology. Additionally, the use of high repetition rate lasers and high-throughput image acquisition also brings the need for advanced methods for handling huge data files and subsequently mining of these data.

With this contribution we report ultra high-speed acquisition times for microprobe MALDI imaging mass spectrometry. A prototype high-speed MALDI-TOF instrument utilizing continuous laser raster sampling was used to acquire 100 μm ion images of a sagittal rat brain tissue section in 10 min. A detailed discussion of the advantages and limitations of continuous laser raster sampling and experimental results highlighting the optimal experimental conditions for ion imaging experiments are presented. With a systematic approach to understanding the fundamentals of continuous laser raster sampling and the development of new instrumentation, the next technological step towards high-throughput MALDI imaging mass spectrometry can be accomplished.

Methods

Sample Preparation

MALDI matrices 2,5-dihydroxybenzoic acid (DHB) and α-cyano-4-hydroxycinnamic acid (CHCA) were purchased from Acros-Organics (Morris Plains, NJ, USA). Angiotensin II (AngII) and all peptides used for external calibration of the instrument were purchased from Sigma-Aldrich (St. Louis, MO, USA). Fresh frozen adult rat brain was purchased from Peel-Freez Biologicals (Rogers, AR, USA). Solutions were prepared using HPLC grade methanol (Fisher Scientific, Fair Lawn, NJ, USA) and Millipore filtered deionized water (Millipore, Bedford, MA, USA). Tissue samples were cryosectioned (12 μm thickness), thaw-mounted on gold-coated plates, and dried in a vacuum dessiccator (~2 h) prior to application of DHB by sublimation (120°C, 50 mTorr, 5.5 min) [21]. For comparison, a serial tissue section was thaw-mounted onto a

glass slide and stained with hematoxylin and eosin (H and E). Continuous laser raster sampling was tested using standard homogenous coatings of AngII (100 nmol/mL) and CHCA (10 mg/ml, 60% methanol/0.1% TFA) spray coated (120°C/10 PSI N_2 sheath gas, 400 µL/min flow rate, four passes) onto gold plates using a TM-Sprayer (LEAP Technologies, Carrboro, NC, USA).

Imaging Mass Spectrometry

All experiments were performed on a prototype MALDI time-of-flight mass spectrometer designed and built by Marvin Vestal and his team at Virgin Instruments (Sudbury, MA, USA). The instrument is a positive mode reflector TOF MS with an effective path length of 3.2 m operated at 8 kV. Briefly, ions are generated using a 349 nm, diode-pumped, frequency-tripled Nd:YLF laser (Spectra-Physics, Santa Clara, CA, USA) capable of operating at laser repetition rates up to 5 kHz. Laser energy is controlled by adjusting the current applied to the diode while keeping laser attenuation constant. All reported laser energies (µJ/pulse) are taken prior to attenuation. Generated Ions are extracted by pulsed acceleration using grid-less ion optics. The ion beam is redirected through two sets of deflector plates on the way to a two-stage ion mirror and detector (0.5 ns electron multiplier). The two deflectors are necessary to move the ion beam from the path of the laser beam that is incident perpendicular to the sample stage and direct the ions to the mirror at the proper angle to maximize resolution. A specified number of laser shots were "hardware" averaged on the acquisition card (model U1082A/AP 240; Acqiris USA, Monroe, NY, USA) prior to writing data to the hard disk. External calibration was performed using a mixture of standard peptides including bradykinin 1–7 (*m/z* 757.85), angiotensin II (*m/z* 1046.54) and [Glu1]-fibrinopeptide B (*m/z* 1570.68) in addition to CHCA clusters (*m/z* 379.09 and *m/z* 568.14). Theoretical and instrumental design considerations have been described previously [22–24].

The instrument is designed to use continuous raster sample interrogation. Ion images of rat brain tissue sections were acquired using both typewriter (acquisition in one lateral direction only) and serpentine (acquisition in both lateral directions) patterns. Tissue images were obtained using a laser repetition rate of 3 kHz (actual: 3056 Hz) at 100 µm spatial resolution as determined vertically by the motor step size between continuous laser raster rows and laterally by setting the stage velocity and hardware average to the appropriate values (see Eq. 1). Best results were observed using a 5 mm/s sample stage velocity and 60 laser shots/spectrum hardware average. Data analysis was done using MiniView analysis software (Virgin Instruments, Sudbury, MA, USA), and all images were color scaled individually from 100%–0% for the relative ion signal intensity.

Lipid identifications were made using mass accuracy data from a MALDI FT-ICR mass spectrometer (9.4 Tesla Apex-Qe; Bruker Daltonics, Billerica, MA, USA) equipped with an Apollo II dual ion source and a 355 nm solid-state laser. External calibration was done using a peptide mixture of bradykinin 1–7, angiotensin II and [Glu1]-fibrinopeptide with the MALDI matrix CHCA. Lipid classifications were determined by comparing mass accuracy data (<1 ppm) with the LIPID MAPS database (Nature Lipidomics Gateway, www.lipidmaps.org).

MALDI Raster Sampling Experiments

To better understand continuous laser raster sampling as a method for MALDI surface interrogation, uniform spray coated layers of AngII/CHCA were analyzed at various sample stage velocities and laser repetition rates. In both cases, data was acquired in a similar fashion as if performing an imaging mass spectrometry experiment by rastering over discrete rectangular areas varying a specific instrumental parameter from one area to another. To understand the relationship between signal intensity and sample stage velocity, all imaged areas were collected using a laser repetition rate of 3 kHz, 5 µJ laser power, 50 laser shots/spectrum, and step size of 200 µm between raster lines. A different sample stage velocity, ranging from 1 to 10 mm/s, was used to sample each area. Similarly, to test the effect laser repetition rate has on signal intensity, areas were sampled using 2 mm/s sample stage velocity, 5 µJ laser power, 50 laser shots/spectrum, and step size of 100 µm between raster lines while varying laser repetition rate for each rectangular area. It should be noted that actual laser repetition rates are slightly different from input values. Optical images of raster lines were taken with an Olympus BX50 20× microscope (Center Valley, PA, USA) and Image-Pro Plus ver. 7 software.

Results and Discussion

High-Speed MALDI TOF Imaging Mass Spectrometry

Using a prototype high-speed MALDI TOF MS built by Virgin Instruments, a sagittal rat brain tissue section (~185 mm^2 total area) was imaged with 100 µm spatial resolution in approximately 10 min using continuous laser raster sampling performed in typewriter mode (see Figure 1). The image has ~19,000 pixels effectively collected at a rate of roughly 30 pixels/s. The instrument was operated with a laser pulse repetition rate of 3 kHz, 60 laser shots/spectrum hardware average, and sample stage velocity of 5 mm/s. It should be noted that under these instrumental conditions, data is actually being collected at a rate of 50 pixels/s, however, the effective rate is reduced because of downtime when using typewriter raster motion. Figure 1a displays a representative spectrum (10 pixel average) showing ions in the low *m/z* range for the experiment. High quality ion images for specific ions can be seen in Figure 1b–e. These specific images were chosen to draw attention to differences

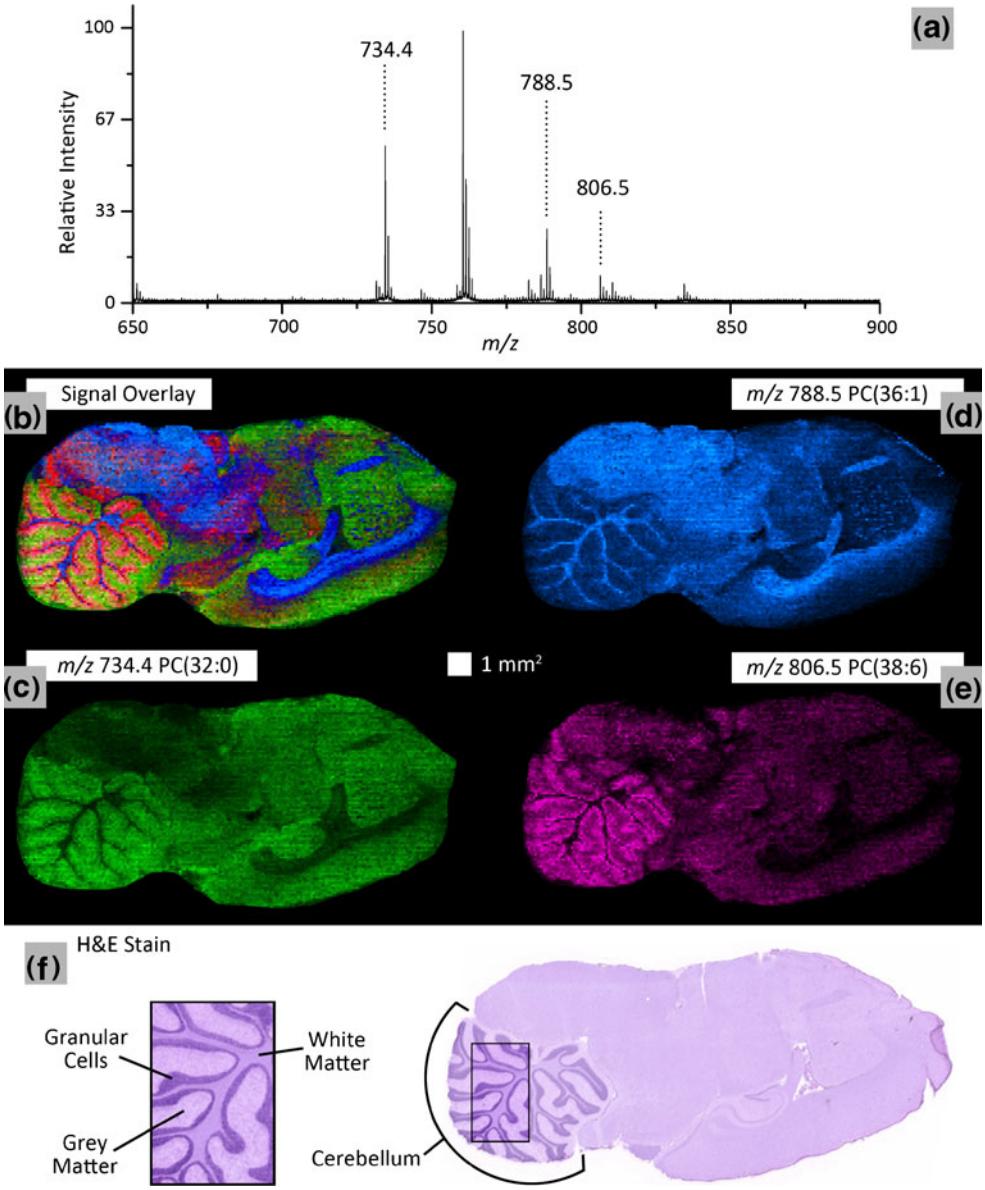

Figure 1. A 100 μm spatial resolution lipid ion image of a sagittal rat brain tissue section using typewriter continuous laser raster sampling acquired in 10 min. (**a**) Representative spectrum is shown. The ion image overlay (**b**) of signal from *m/z* 734.4 PC(32:0) (**c**), *m/z* 788.5 PC(36:1) (**d**), and *m/z* 806.5 PC(38:6) (**e**) highlights the differentiation of the spatial distributions for the selected ions. These results correlate to the H and E stained serial tissue section highlighting structural difference between grey matter, white matter and granular cells in the cerebellum (**f**). Important instrumental parameters: 3 kHz laser repetition rate, 5 mm/s sample stage velocity, and 60 laser shots/spectrum hardware average

in spatial distribution that are particularly apparent in the cerebellum region of the rat brain. The H and E stained histologic rat brain tissue section similar to that used for IMS analysis seen in Figure 1f highlights the structural differences between grey matter, white matter, and granular cells of the cerebellum. The MALDI IMS results add molecular information to the histology as shown for the *m/z* 734.4 (green, Figure 1c), *m/z* 788.5 (blue, Figure 1d) and *m/z* 806.5 (pink, Figure 1e) ions. All three ions were identified by mass accuracy to be phosphatidylcholines with varying fatty acid chain lengths and degrees of unsaturation. The overlay of all three color channels (Figure 1b) emphasizes the differences in spatial distributions of the three ions showing localization to the grey matter [*m/z* 734.5 PC(32:0)], white matter [*m/z* 788.5 PC(36:1)] and granular cells [*m/z* 806.5 PC(38:6)] of the cerebellum respectively. These results are consistent with those previously reported in the literature [25, 26]. The ability to acquire high quality ion images from a tissue section of this size with 100 μm spatial resolution in 10 min is a major advancement for imaging mass spectrometry and MALDI TOF MS in general.

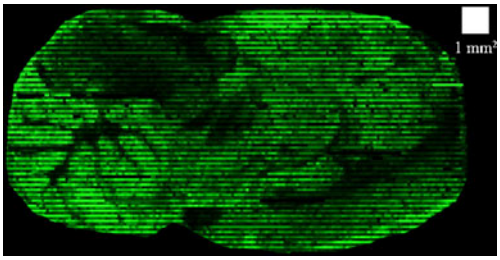

Figure 2. Low quality ion image (*m/z* 734.4) of a sagittal rat brain tissue section using serpentine raster sampling showing "stripes." Image quality is diminished by striping caused by differences in ion signal intensity dependent on the direction of sample stage motion. Important instrumental parameters: 3 kHz laser repetition rate, 6 mm/s sample stage velocity, 50 laser shots/spectrum hardware average, 100 µm spatial resolution

An interesting observation made during the testing of the instrument for imaging experiments was that continuous laser raster sampling needed to be performed using typewriter motion to acquire high quality images. Generally, continuous laser raster sampling can be done by moving the sample though the incident laser beam in two ways: typewriter and serpentine motion. In typewriter mode, data is acquired while moving the sample stage in only one direction. Following the completion of one raster line the sample stage moves such that the laser passes directly over the line that was just completed to the starting point of that raster line before stepping down to the next line. In serpentine mode, data is acquired in both directions stepping down to the next line immediately following the completion of a raster line. Although serpentine continuous laser raster sampling would naturally take less time than typewriter motion, we have found that images acquired in serpentine mode are of lower quality due to "stripes" caused by regular differences in ion signal intensity determined by the direction of sample stage motion during acquisition (see Figure 2). The ion image, represented in this case for the *m/z* 734.4 ion, was acquired in 6 min using serpentine motion with the same instrumental parameters as for the high quality image shown in Figure 1. Although the exact cause of this artifact is unclear, we speculate that differences in ion signal intensity may be due to slight differences in sample stage velocity from directional inconsistencies in the sample stage motors or from directional differences of ion emission. Variance in sample stage velocity, as will be discussed in detail in the next section, would affect laser spot overlap and, in turn, signal intensity. Alternatively, the slope caused by continuous laser raster sampling from the gradient of overlapping laser shots may affect the direction of ion emission from the surface. The direction of the slope is dependent upon the scanning direction perhaps causing differences in ion transfer efficiencies. The extra time resulting from typewriter motion is outweighed by the increased quality of the ion images collected. It is unclear whether this phenomenon is unique to our instrument or is generally applicable to high-speed data acquisition, nevertheless as a precautionary note, we recommend checking this issue when using continuous laser raster sampling. Additionally, if a future generation instrument has MS/MS capabilities, typewriter motion sampling may provide the ability to acquire parent ion images and targeted MS/MS data in the same amount of time by performing fragmentation experiments on residual sample while the sample stage is moving back to the starting position for each raster line.

Continuous Laser Raster Sampling

Continuous laser raster sampling is a relatively new surface interrogation technique that has been shown to significantly increase the speed of MALDI mass spectrometry acquisition making it ideal for IMS experiments [20]. This technique involves simply moving the sample stage laterally while maintaining a constant laser repetition rate and sample stage velocity. The graphic shown in Figure 3 highlights the significant amount of laser shot overlap that occurs for fairly moderate experimental conditions. For instance, after an initial distance roughly equal to the laser diameter, a sample moving 5 mm/s through the path of a laser beam with a 50 µm diameter and

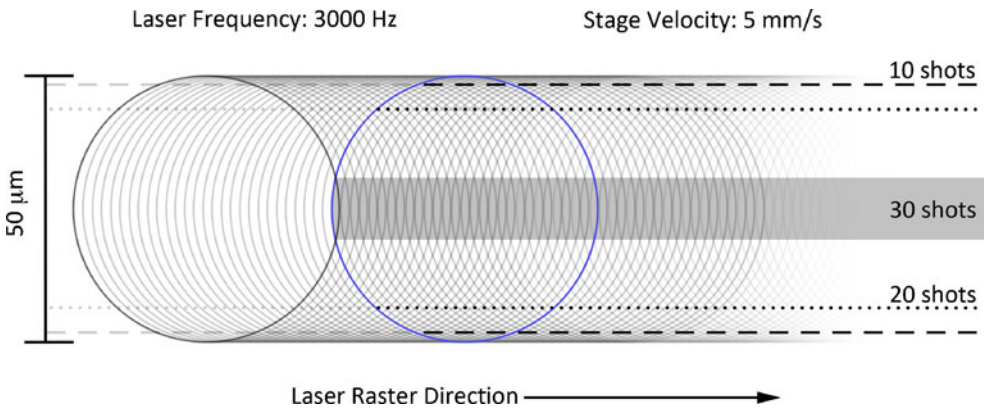

Figure 3. An illustration of continuous laser raster MALDI sampling highlighting the number of laser shots/unit area for a representative laser frequency (3 kHz), laser spot diameter (50 µm) and stage velocity (5 mm/s). After an initial distance roughly equal to the diameter of the laser beam, the sampling conditions become constant (blue circle) with a maximum of 30 shots/unit area. Laser shot overlap decreases for areas further away from the center of the raster path (grey bar)

3 kHz pulse repetition rate will have a maximum laser shot overlap of 30 shots/unit area. Laser shot overlap decreases further away from the center of the raster path due to the circular shape of the incident laser beam. In Figure 3, the black circle denotes the first laser shot and the blue circle represents the point at which sampling conditions become constant. The number of laser shots/unit area is calculated by simply determining the time it takes to move the sample stage a distance equal to the laser diameter and relating that to the laser repetition rate as seen in Eq. 2

$$\text{Laser Shots/Unit Area} = f_{rep}\left(\frac{d}{v_{stage}}\right) \quad (2)$$

where f_{rep} is the laser pulse repetition rate, d is the laser beam diameter, and v_{stage} is the sample stage velocity. It should be noted that "unit area" is unitless because the units used to describe area within, for example, the center of the laser raster path (grey bar, Figure 3) are inconsequential to the number of overlapping laser shots and, in turn, the number of laser shots/unit area.

Understanding the relationship between laser shots/unit area and experimental conditions such as sample stage velocity and laser repetition rate is extremely important for optimizing continuous laser raster sampling for imaging mass spectrometry. An early observation made while using our prototype high-speed TOF mass spectrometer was the improved signal intensity with higher sample stage velocity. This suggested that severe oversampling may be a problem at slower rates. To further explore this, theoretical plots for maximum laser shots/unit area (center of raster path) as a function of sample stage velocity, laser repetition rate and laser spot diameter (Figure 4a, b, and c, respectively) were generated. The inverse relationship (Eq. 2) with sample stage velocity causes the number of laser shots/unit area to increase rapidly for slower velocities as shown for a 50 µm diameter laser beam in Figure 4a. Stage velocity becomes particularly important at very high laser repetition rates (10–20 kHz). For example, even when moving the sample stage 10 mm/s there are 100 laser shots/unit area when operating a 50 µm diameter laser at a 20 kHz pulse repetition rate. Similar arguments can be made when relating laser shots/unit area to laser repetition rate (Figure 4b). In this case, the number of laser shots/unit area increases linearly with respect to pulse repetition rate again showing significant laser spot overlap, particularly at slow sample stage velocities. Using a laser beam with a diameter of 50 µm, Figure 4b shows that to operate a laser at pulse repetition rates ≥10 kHz the sample stage would need to be moved at velocities greater than 10 mm/s to have ≤50 laser shots/unit area. From a practical standpoint this may not be reasonable due to mechanical limitations of most sample stage motors. Further, operating at such high velocities and accelerating and decelerating rapidly to such high speeds could significantly decrease the lifetime of sample stage components. Therefore, for moderate laser beam diameters (20–80 µm) laser pulse repetition rates <5 kHz may be preferred.

As imaging mass spectrometry technology advances, high repetition rate lasers will become essential for high-resolution imaging experiments. Figure 4c shows the relationship between laser shots/unit area and laser beam diameter at different laser repetition rates at a fixed sample stage velocity (5 mm/s). It is apparent from this plot that as the technology

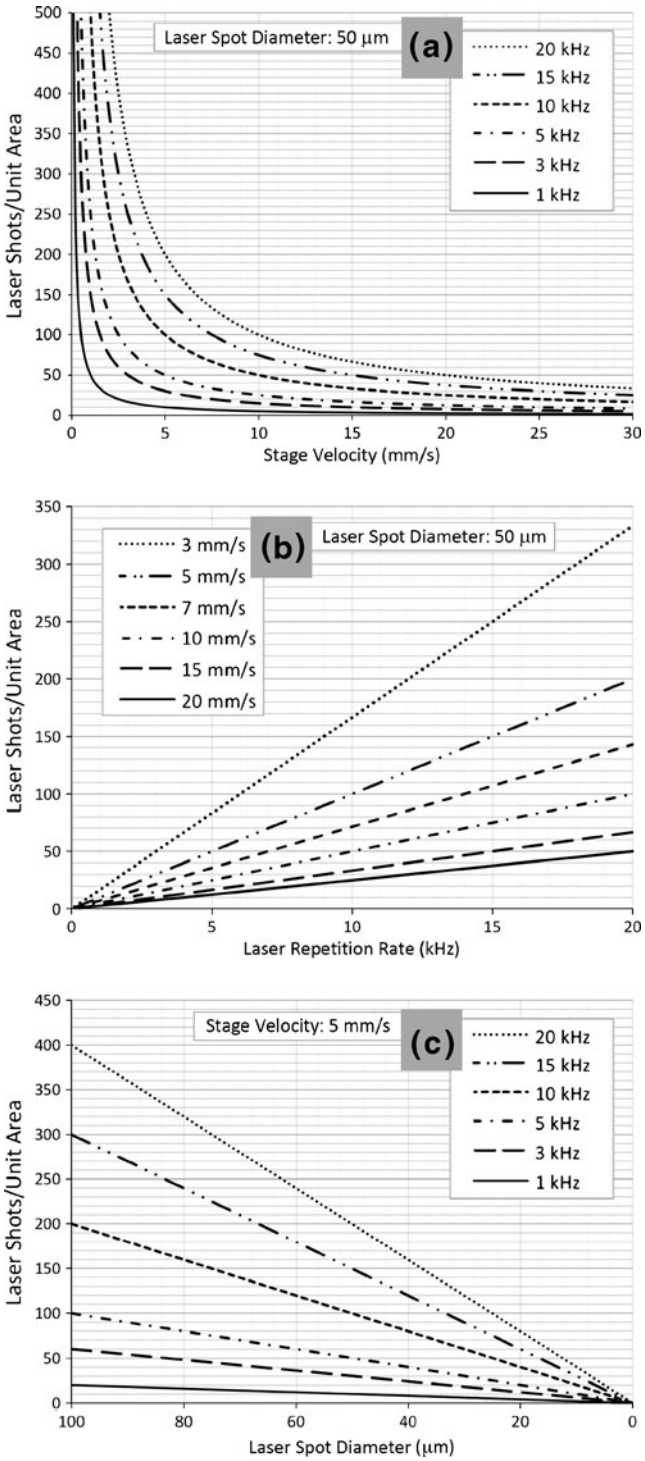

Figure 4. Theoretical calculations for the number of laser shots/unit area as a function of (**a**) sample stage velocity, (**b**) laser pulse repetition rate and (**c**) laser beam diameter. 50 µm laser beam diameter was assumed for **a** and **b**. A sample stage velocity of 5 mm/s was used for plot **c**

moves towards using smaller laser spot sizes (<10 μm diameter) to acquire higher spatial resolution ion images laser spot overlap will not be significant. High pulse repetition rate lasers (>10 kHz) can then be used to acquire images quickly with very little detriment to signal intensity from substantial oversampling. There are, however, new problems that arise when using such high laser repetition rates. For example, a sample moving through the path of a 5 μm diameter laser operating at a pulse repetition rate of 20 kHz at 5 mm/s will have a laser spot overlap of 20 laser shots/unit area. Assuming the pulsed extraction voltages can be operated at 20 kHz, acquiring a 5 μm spatial resolution ion image using these experimental conditions (20 kHz laser repetition rate, 5 mm/s stage velocity, 20 laser shots/spectrum hardware average) would require an acquisition rate of 1000 spectra/s, which is not currently attainable. To circumvent this issue while maintaining 20 kHz laser repetition rates and the same spatial resolution the hardware average would need to be increased and the sample stage velocity decreased (Eq. 1). Unfortunately, this would then potentially cause ion signal intensity to diminish from increasing laser shot overlap. Laser repetition rates >10 kHz may not be necessary and in many cases may actually non-optimal due to either oversampling or the inability to save data fast enough.

To further study these issues, experiments were designed to monitor ion signal intensity as a function of sample stage velocity and laser repetition rate using continuous laser raster sampling. The experiments involved acquiring ion images of sequential rectangular areas on a homogeneous standard coating (angiotensin II, *m/z* 1046.5) while varying specific instrumental parameters. Results showing variance in AngII signal intensity as a function of sample stage

Table 1. Angiotensin II (*m/z* 1046.5) Signal Intensity as a Function of Stage Velocity Using Raster Sampling. Ion Image Areas were Averaged and Compared to Calculated Values for Spatial Resolution and Shots/Unit Area. Loss of Signal at Slower Sampling Speed is Shown to Correlate to Oversampling as Confirmed by Optical Images

Velocity (mm/s)	20x Optical Image[a] (1 Raster Line)	AngII Signal Intensity[b] (3 Raster Lines)	Avg. Peak Area (Arbitrary Units)	Spatial Resolution[c] (μm)	Shots/Unit Area[d]
10		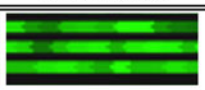	269369	164	15.3
9	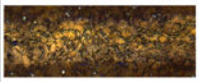	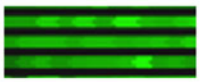	221029	147	17.0
8		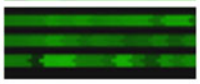	167846	131	19.1
7		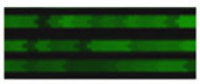	144492	114	21.8
6	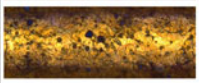	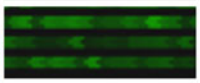	139911	98	25.5
5		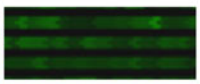	133335	82	30.6
4			129743	65	38.2
3		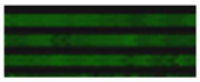	126805	49	51.0
2			115681	33	76.5
1		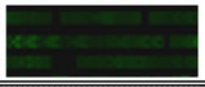	66961	16	152.9
	Plots highlight trends as a function of stage velocity		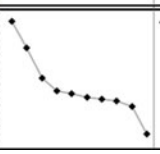	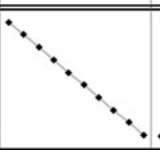	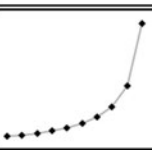

Instrumental Parameters - Laser Repetition Rate: 3058 Hz, 50 Laser Shots/Spectrum, Laser Power: 5 μJ
[a]Total optical image area is 70 × 190 μm.
[b]Step size between raster lines: 200 μm.
[c]Effective spatial resolution only in horizontal dimension.
[d]Maximum laser shot overlap (center of raster path). Area, in this case, is a unitless value.

velocity can be found in Table 1. This experiment was done while maintaining a laser repetition rate of 3 kHz, 5 μJ laser power and hardware average of 50 laser shots/spectrum. It should be noted that because the laser repetition rate and hardware average are held constant the effective lateral spatial resolution decreases with decreasing sample stage velocities (See Eq. 1). Ion image areas show a significant decrease in signal intensities (AngII signal intensity and average peak area, Table 1) with decreasing sample stage velocities. The 20× optical images of single continuous laser raster lines suggest that diminishing ion signal results from severe oversampling occurring as the number of laser shots/unit area rapidly increases with decreasing sample stage velocity. Particularly for stage velocities <4 mm/s, it can be seen that the sample and matrix are completely ablated as highlighted by the exposure of the gold coated MALDI target (bright areas) in the optical images. The widening of the complete ablation area is a result of (1) the circular shape of the incident laser beam, and (2) the Gaussian nature of the laser beam energy profile for solid state lasers. We suggest that with a high degree of laser spot overlap, only the leading edge of the laser beam produces ions. For the sake of argument, if we assume all sample and matrix is ablated after 30 laser shots, then for the instrumental conditions of this experiment (3 kHz laser repetition rate and 50 μm laser diameter) a sample stage velocity of 1 mm/s would result in 80% of the incident laser beam irradiating an area where no sample remains. This value is simply estimated by calculating the time it takes for the laser to fire 30 times (1×10^{-2} s) and relating that to the sample stage velocity (1 mm/s) to determine how far the stage moves before it is assumed that all sample is completely ablated (10 μm). If only the first 10 μm of a 50 μm laser spot irradiates analyte then 80% of that beam samples nothing. Although the actual case is much more complicated because of the laser beam shape and energy profile, when using high pulse repetition rate lasers for continuous laser raster sampling our results suggest that either the sample stage needs to be moved with high velocity or the laser beam diameter needs to be sufficiently small to avoid signal depletion due to oversampling.

Similar results were found for ion signal dependence on laser repetition rate as seen in Table 2. For this experiment, a

Table 2. Angiotensin II (*m/z* 1046.5) Signal Intensity as a Function of Laser Repetition Rate Using Raster Sampling. Ion Image Areas were Averaged and Compared to Calculated Values for Spatial Resolution and Shots/Unit Area. Loss of Signal at Higher Repetition Rates is Shown to Correlate to Oversampling as Confirmed by Optical Images

Repetition Rate (Hz)	20x Optical Image[a] (1 Raster Line)	AngII Signal Intensity[b] (4 Raster Lines)	Avg. Peak Area (Arbitrary Units)	Spatial Resolution[c] (μm)	Shots/Unit Area[d]
1017	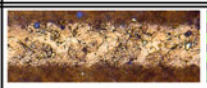	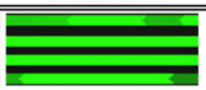	338259	197	25.4
1526		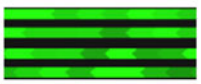	296824	131	38.2
2035		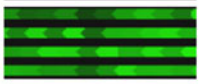	276161	98	50.9
2441		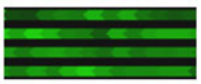	212455	82	61.0
3058		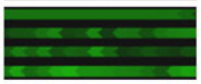	180339	65	76.5
3488		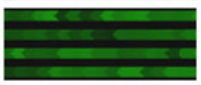	169844	57	87.2
4069		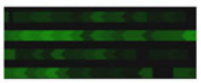	109105	49	101.7
4883			42376	41	122.1
	Plots highlight trends as a function of laser repetition rate.		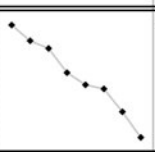	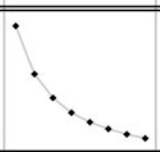	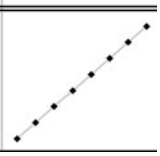

Instrumental Parameters - Sample Stage Velocity: 2 mm/s, 50 Laser Shots/Spectrum, Laser Power: 5 μJ
[a]Total optical image area is 70 × 190 μm.
[b]Step size between raster lines: 200 μm.
[c]Effective spatial resolution only in horizontal dimension.
[d]Maximum laser shot overlap (center of raster path). Area, in this case, is a unitless value.

2 mm/s sample stage velocity, 50 laser shots/spectrum hardware average, and 5 μJ laser energy were maintained while varying laser repetition rate. In this case, because sample stage velocity and hardware average were constant, effective lateral spatial resolution decreases with increasing laser repetition rate (Eq. 1). Again, we see a significant decrease in ion signal intensity (AngII signal intensity and average peak area, Table 2) with increasing laser repetition rate that seems to correlate to oversampling as the number of laser shots/unit area increases. The 20× optical images show complete ablation begins where laser spot overlap is at its highest (center area of the raster line, grey bar, Figure 3) just below 40 laser shots/unit area, comparable to observations made for the previous sample stage velocity experiment (Table 1). Making the same assumptions as previously done, when operating the laser near 5 kHz (4883 Hz) and moving the stage 2 mm/s results in roughly 76% of the laser beam being incident on an area where sample has already been completely ablated. This severe oversampling leads to the poor ion signal observed with high laser repetition rates at slow sample stage velocities.

The experimental results described above are consistent with the hypothesis that for continuous laser raster sampling severe oversampling can occur under certain experimental conditions, leading to low ion signal intensities. As highlighted by the theoretical calculations (Figure 4a and b), with decreasing sample stage velocity and/or increasing laser repetition rate laser spot overlap increases rapidly, leading to poor spectra quality from oversampling. Although the experimental results are expected to vary slightly for different MALDI matrices, matrix deposition methods, and sample thickness, our results suggest that to prevent ion signal degradation experimental conditions should be such that laser shot overlap is <50 laser shots/unit area. These experiments set the framework for using continuous laser raster sampling to generate high quality ion images for MALDI imaging mass spectrometry.

Conclusions

As imaging mass spectrometry adapts to handle higher spatial resolution and larger sample area applications time and throughput become significant issues. We have used a prototype high-speed MALDI TOF mass spectrometer with continuous laser raster sampling capable of acquiring ion images more than 10× faster than commercially available MALDI imaging mass spectrometers. Sagittal rat brain lipid ion images acquired with 100 μm spatial resolution were collected in 10 min using a laser repetition rate of 3 kHz in typewriter motion raster sampling. These images were effectively acquired at a rate of 30 pixels/s. A systematic study of continuous laser raster sampling showed that poor ion signal intensity can result from severe oversampling due to exceedingly high laser repetition rates and/or slow sample stage velocity. These results suggest that for optimal performance, laser shot overlap should not exceed 50 laser shots/unit area. Theoretical calculations suggest that for moderate laser diameters (20–80 μm), laser repetition rates <5 kHz may be preferred and laser repetition rates >10 kHz can be unfavorable, even for small laser beam diameters, because of oversampling and the inability to currently write data to disc at sufficiently high rates. These results help in the development of the next generation of MALDI imaging mass spectrometry technology and its ability to handle the new technical and biological challenges imposed by speed, spatial resolution, and sample size.

Acknowledgments

The authors gratefully acknowledge financial support from NIH grants 5R01GM58008–12 and 1P41 031461-01. They thank Marvin Vestal, Matt Gabeler-Lee, Kevin Hayden, George Mills, and P. Jane Gale at Virgin Instruments for their help and advice.

References

1. Caprioli, R.M., Farmer, T.B., Gile, J.: Molecular Imaging of Biological Samples: Localization of Peptides and Proteins using MALDI-TOF MS. *Anal. Chem.* **69**, 4751–4760 (1997)
2. Amstalden van Hove, E.R., Smith, D.F., Heeren, R.M.A.: A Concise Review of Mass Spectrometry Imaging. *J. Chromatogr. A* **1217**, 3946–3954 (2010)
3. McDonnell, L.A., Corthals, G.L., Willems, S.M., van Remoortere, A., van Zeijl, R.J.M., Deelder, A.M.: Peptide and Protein Imaging Mass Spectrometry in Cancer Research. *Journal of Proteomics* **73**(10), 1921–1944 (2010)
4. Svatos, A.: Mass Spectrometric Imaging of Small Molecules. *Trends Biotechnol.* **28**, 425–434 (2010)
5. Cornett, D.S., Reyzer, M.L., Chaurand, P., Caprioli, R.M.: MALDI Imaging Mass Spectrometry: Molecular Snapshots of Biochemical Systems. *Nat. Methods* **4**, 828–833 (2007)
6. McDonnell, L.A., Heeren, R.M.A.: Imaging Mass Spectrometry. *Mass Spectrom. Rev.* **26**, 606–643 (2007)
7. Guenther, S., Koestler, M., Schulz, O., Spengler, B.: Laser Spot Size and Laser Power Dependence of Ion Formation in High Resolution MALDI Imaging. *Int. J. Mass Spectrom.* **294**, 7–15 (2010)
8. Jun, J.H., Song, Z., Liu, Z., Nikolau, B.J., Yeung, E.S., Lee, Y.J.: High-Spatial and High-Mass Resolution Imaging of Surface Metabolites of Arabidopsis Thaliana by Laser Desorption-Ionization Mass Spectrometry using Colloidal Silver. *Anal. Chem.* **82**, 3255–3265 (2010)
9. Chaurand, P., Schriver, K.E., Caprioli, R.M.: Instrument Design and Characterization for High Resolution MALDI-MS Imaging of Tissue Sections. *J. Mass Spectrom.* **42**, 476–489 (2007)
10. Reyzer, M.L., Chaurand, P., Angel, P.M., Caprioli, R.M.: Direct Molecular Analysis of Whole-Body Animal Tissue Sections by MALDI Imaging Mass Spectrometry. *Methods Mol. Biol.* **656**, 285–301 (2010)
11. Solon, E.G., Schweitzer, A., Stoeckli, M., Prideaux, B.: Autoradiography, MALDI-MS, and SIMS-MS Imaging in Pharmaceutical Discovery and Development. *AAPS J.* **12**, 11–26 (2010)
12. Trim, P.J., Henson, C.M., Avery, J.L., McEwen, A., Snel, M.F., Claude, E., Marshall, P.S., West, A., Princivalle, A.P., Clench, M.R.: Matrix-Assisted Laser Desorption/Ionization-Ion Mobility Separation-Mass Spectrometry Imaging of Vinblastine in Whole Body Tissue Sections. *Anal. Chem.* **80**, 8628–8634 (2008)
13. Stoeckli, M., Staab, D., Schweitzer, A., Gardiner, J., Seebach, D.: Imaging of a Î²-Peptide Distribution in Whole-Body Mice Sections by MALDI Mass Spectrometry. *J. Am. Soc. Mass Spectrom.* **18**, 1921–1924 (2007)
14. Djidja, M., Claude, E., Snel, M.F., Francese, S., Scriven, P., Carolan, V., Clench, M.R.: Novel Molecular Tumor Classification using MALDI-Mass Spectrometry Imaging of Tissue Micro-Array. *Anal. Bioanal. Chem.* **397**, 587–601 (2010)

15. Morita, Y., Ikegami, K., Goto-Inoue, N., Hayasaka, T., Zaima, N., Tanaka, H., Uehara, T., Setoguchi, T., Sakaguchi, T., Igarashi, H., Sugimura, H., Setou, M., Konno, H.: Imaging Mass Spectrometry of Gastric Carcinoma in Formalin-Fixed Paraffin-Embedded Tissue Microarray. *Cancer Sci.* **101**, 267–273 (2010)
16. Groseclose, M.R., Massion, P.P., Chaurand, P., Caprioli, R.M.: High-Throughput Proteomic Analysis of Formalin-Fixed Paraffin-Embedded Tissue Microarrays using MALDI Imaging Mass Spectrometry. *Proteomics.* **8**, 3715–3724 (2008)
17. Karas, M., Hillenkamp, F.: Laser Desorption Ionization of Proteins with Molecular Masses Exceeding 10,000 Daltons. *Anal. Chem.* **60**, 2299–2301 (1988)
18. Holle, A., Haase, A., Kayser, M., Hoehndorf, J.: Optimizing UV Laser Focus Profiles for Improved MALDI Performance. *J. Mass Spectrom.* **41**, 705–716 (2006)
19. Trim, P.J., Djidja, M., Atkinson, S.J., Oakes, K., Cole, L.M., Anderson, D.M.G., Hart, P.J., Francese, S., Clench, M.R.: Introduction of a 20 kHz Nd:YVO4 Laser into a Hybrid Quadrupole Time-of-Flight Mass Spectrometer for MALDI-MS Imaging. *Anal. Bioanal. Chem.* **397**, 3409–3419 (2010)
20. Simmons, D. A. Improved MALDI-MS Imaging Performance using Continuous Laser Rastering. *Applied Biosystems Technical Note.* **2008**.
21. Hankin, J.A., Barkley, R.M., Murphy, R.C.: Sublimation as a Method of Matrix Application for Mass Spectrometric Imaging. *J. Am. Soc. Mass Spectrom.* **18**, 1646–1652 (2007)
22. Vestal, M.L.: Modern MALDI Time-of-Flight Mass Spectrometry. *J. Mass Spectrom.* **44**, 303–317 (2009)
23. Vestal, M., Hayden, K.: High Performance MALDI-TOF Mass Spectrometry for Proteomics. *Int. J. Mass Spectrom.* **268**, 83–92 (2007)
24. Vestal, M. L.; Hayden, K. M. High-Performance MALDI-TOF Mass Spectrometry. *Proceedings of the ASMS Conference on Mass Spectrometry and Allied Topics*, Indianapolis, USA, June (2007)
25. Jackson, S.N., Wang, H.J., Woods, A.S.: In Situ Structural Characterization of Phosphatidylcholines in Brain Tissue using MALDI-MS/MS. *J. Am. Soc. Mass Spectrom.* **16**, 2052–2056 (2005)
26. Hankin, J.A., Murphy, R.C.: Relationship between MALDI IMS Intensity and Measured Quantity of Selected Phospholipids in Rat Brain Sections. *Anal. Chem.* **82**, 8476–8484 (2010)